

The influence of collision and vibrational energy on the reaction of CH_3CHO^+ with acetylene

Ho-Tae Kim, Jianbo Liu, and Scott L. Anderson

Department of Chemistry, University of Utah, Salt Lake City, Utah 84112-0850

(Received 22 January 2001; accepted 21 February 2001)

Reaction of acetaldehyde cations with acetylene has been studied as a function of collision energy and acetaldehyde vibrational state. CH_3CHO^+ is state selected by resonance-enhanced multiphoton ionization, and scattered from C_2H_2 in a guided ion beam instrument. We have also calculated the structures and energetics of 11 different hydrogen-bonded, covalently bound, and coordination complexes, some of which are clearly intermediates in the reaction. From the product distribution, it is clear that some of the most stable complexes do not participate in the reaction. The most exoergic product observed corresponds to CH_3 elimination from a covalently bound complex, but this channel accounts for no more than a few percent of the total reaction signal. The dominant channel is hydrogen transfer ($\text{CH}_3\text{CO}^+ + \text{C}_2\text{H}_3$), which proceeds with >73% efficiency at low energies, dropping to a near constant 30% at energies above 1 eV. Product recoil velocity distributions indicate that this channel is complex mediated at low energies, switching to direct scattering at high energies. The hydrogen transfer reaction is weakly affected by reactant vibration, including ν_3 , the aldehyde CH stretch. Methyl elimination is strongly, but nonmode specifically inhibited by vibration. © 2001 American Institute of Physics. [DOI: 10.1063/1.1364684]

I. INTRODUCTION

The reaction dynamics of even small polyatomic systems can be quite complicated because there are typically many local minima and transition states, and several competing product channels, possibly with several mechanisms contributing to each. We have found that a rather detailed picture of the dynamics can often be inferred by combining measurements of vibrational mode effects on reactivity and product branching, measurements of product recoil velocity distributions, *ab initio* probing of the reaction path energetics, and RRKM calculations of complex lifetimes and decomposition pathways.¹⁻⁶ Vibrational mode effects provide insight into the dynamics and transition states in the early parts of collision, before collisional interactions can scramble the initial excitation. The collision and vibrational energy dependence of the product branching gives information about interchannel competition and further insight into the factors that control reactivity. Product recoil velocity distributions probe the intimate collision dynamics, giving evidence of the collision time scale, and types of scattering events that dominate for different product channels. Recoil distributions also probe partitioning of available energy into the internal versus relative degrees of freedom. *Ab initio* calculations give geometry and energetics for complexes and transition states, and RRKM calculations provide complex lifetimes and decay branching information.

One interesting class of systems are those where covalent intermediate complexes exist, which may play an important role in the reaction mechanism. For example, in the reaction of C_2H_2^+ with CH_4 , covalent C_3H_6^+ complexes mediate the dominant reactions, and allow isotope scrambling and other complicated rearrangements. This system also has several forms of weakly bound coordination complexes, and

these appear to be critical in mediating both direct reactions and transition to the covalently bound complexes.^{1,7,8} On the other hand, in the reactions of C_2H_2^+ with CH_3OH^5 and NH_3 ,³ the reactants do not explore the covalently bound regions of the potential surface, even though the covalent complexes in those systems are even more strongly bound than in the $\text{C}_2\text{H}_2^+ + \text{CH}_4$ case. There appear to be no barriers blocking access to the covalent regions of the potential surfaces,^{9,10} leading to the conclusion that dynamics, rather than energetics, control the reaction mechanism, even at the lowest energies.

Here we report a study of the reaction of CH_3CHO^+ with C_2H_2 —a system that can form both strongly bound covalent and weakly bound coordination complexes. As we will show, the system appears to explore some covalently bound regions of the potential surface, but avoids the most strongly bound covalent complexes. Despite the strong binding in the covalent complexes, the weakly bound regions of the potential surface are more important in controlling the reaction.

Vibrational mode-selectively excited CH_3CHO^+ reactants are prepared by resonance-enhanced multiphoton ionization (REMPI), using excitation routes recently reported.¹¹ Several different combinations of vibrational modes can be selected, with energies up to 0.44 eV. The energetics of the reaction are summarized in Fig. 1. Energetics for reactants, products, and some covalently bound $\text{C}_4\text{H}_6\text{O}^+$ species are taken from the compilation of Lias *et al.*¹² Structures and energetics of the coordination complexes are from *ab initio* calculations, discussed below.¹³ The complexes can be characterized as reactantlike (A-C), productlike (J,K), and other (D-I). A combination of experimental results with *ab initio* and RRKM calculations suggests that two distinct types of

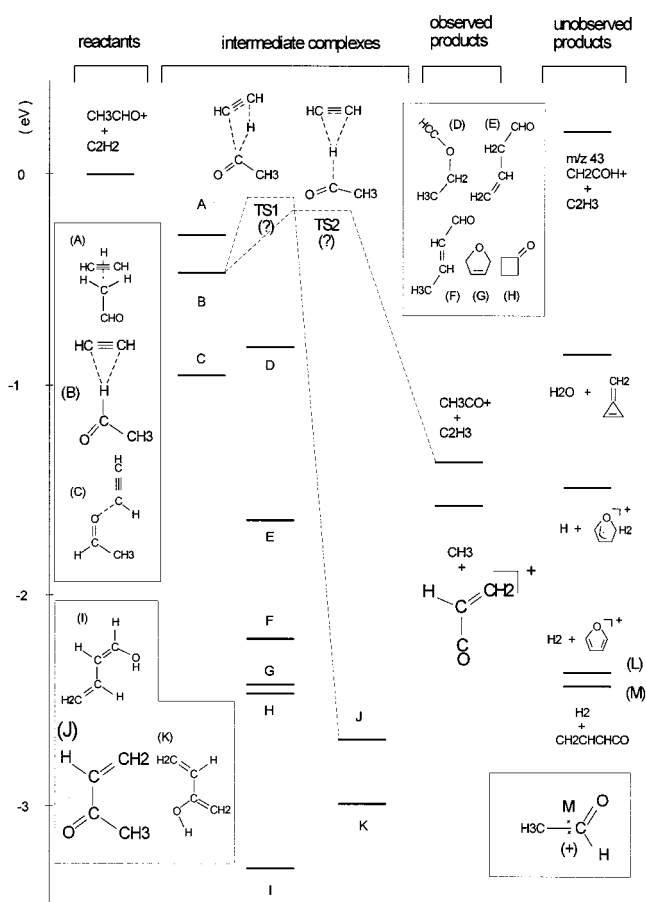


FIG. 1. Schematic reaction coordinate for the reaction of CH_3CHO^+ with C_2H_2 . Energetics are from a combination of experimental sources and *ab initio* calculations (see text).

intermediate complexes are important in accounting for changes in the reaction dynamics with energy. Product branching appears to be determined by the competition between direct reaction and isomerization pathways out of the reactantlike complexes.

II. EXPERIMENT AND CALCULATION

The guided-ion-beam (GIB) tandem mass spectrometer used in this study has been described previously,¹ along with the operation, calibration, and data analysis procedures. Vibrationally state-selected beams of CH_3CHO^+ were prepared by REMPI of a pulsed, seeded supersonic beam of CH_3CHO . The gas mixture for the beam was prepared by vaporizing liquid acetaldehyde (Fisher Scientific, 99.5%) at

about 30 °C and entraining the vapor in 200 psi of helium carrier (Matheson 99.9%). The mixture was expanded through a pulsed valve, collimated by a skimmer, then introduced to the ionization region.

The REMPI procedures used to prepare state-selected CH_3CHO^+ cations have been discussed previously in detail.¹¹ The vibrational states, or mixtures of states, resulting from each REMPI transition are listed in Table I. The origin, 10^1 , 9^1 , and 3^1 transitions generate ions with >80% in a single vibrational state, with the remaining ions also having excitation of the dominant mode. The two other transitions produce cations with no dominant state, but with one mode or combinations thereof, dominating the distribution. For the present system, there are no mode-specific effects, therefore we will not emphasize the nature of the different reactant states. We note only that ν_3 is the aldehyde CH stretch, i.e., the stretch of the bond being broken in the hydrogen transfer reaction. Note that CH_3CHO^+ has low-lying isomers, however, the vibrational energies selected are all well below the isomerization activation barriers,^{14–18} thus the parent ion should be stable.

The energy spread of the ion beam is reduced by a combination of focusing in the quadrupole ion guide and TOF gating after the quadrupole ion guide. The reactant ions are then injected into a short segment of octapole ion guide, where they pass through a scattering cell containing C_2H_2 vapor. For these experiments we used neat C_2H_2 (95%, Matheson) purified by passage through a dry ice/acetone trap to remove solvent. The inlet valve is kept at about 70 °C to avoid freezing C_2H_2 in the valve orifice. The scattering cell pressure is kept at 4.5×10^{-5} Torr and monitored by a capacitance manometer. Product ions and unreacted CH_3CHO^+ are collected by the octapole, then guided into a second, longer octapole, where TOF analysis can be used to measure both primary and product ion velocity distributions. The ions are finally mass analyzed by a quadrupole mass spectrometer, and counted.

Nascent CH_3CHO^+ produced by 2+1 REMPI can absorb an additional photon and fragment to $\text{HCO}^+ + \text{CH}_3$ or $\text{CH}_3\text{CO}^+ + \text{H}$. The HCO^+ fragments are completely eliminated by time-of-flight (TOF) gating, and CH_3CO^+ in the CH_3CHO^+ beam is kept below 2%. At this level, the contaminant is not a problem, as the very stable CH_3CO^+ ion is unreactive with C_2H_2 , because all product channels would be more than 4 eV endoergic. The only exception is the hydrogen transfer channel for CH_3CHO^+ produced by pumping through the 3^1 transition, where the parent intensity

TABLE I. Summarized results of REMPI-PES experiment with CH_3CHO .

Intermediate B state level	Ion states observed in PES	Average ion vibrational energy (meV)
origin	vibrationless (100%)	0
10^1	10^1 (100%)	45
9^1	9^1 (47%); $9^1 10^1$ (26%); 8^1 (27%)	130
6^1 or 7^1	$6^1 10^1$ (29%); $14^1 9^1$ (37%); $6^1 15^1$ (34%)	194
5^1	$5^1 10^1$ (90%); 5^1 (10%)	222
3^1	$3^1 10^2$ (80%); $3^1 15^2$ (15%); 3^1 (5%)	439

is very low. To eliminate any possible problems with interference from the CH_3CO^+ fragment ion in the beam, a set of experiments was performed with a modified source arrangement. In these experiments, the quadrupole ion guide was replaced by a conventional quadrupole mass filter, completely removing the CH_3CO^+ background. The mass filter source was not used for all experiments because the translational energy spread of the ion beam (<0.2 eV FWHM) is badly broadened (~ 0.5 eV) by interaction with fringe fields in the mass filter. With the exception of energy resolution, the two sets of data are identical within the scatter of the data.

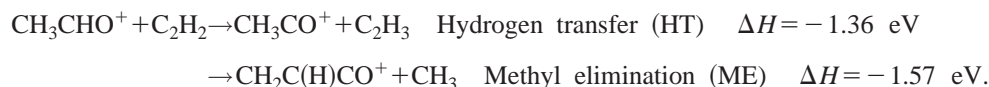
To aid in reaction coordinate interpretation and to get energetic information, *ab initio* calculations were performed using MP2 and B3LYP theories with 6-31G* and 6-311++G** basis sets, using GAUSSIAN 98.¹³ Geometries were optimized calculating both gradients and force con-

stants at each step, and the geometries and relative stabilities at the MP2 and B3LYP levels are consistent. Reactant, product, and complex energies were also calculated at the G3 level of theory. RRKM rate calculations were done with the program of Zhu and Hase¹⁹ using its direct state count algorithm, scaled frequencies from our B3LYP/6-311++G** calculations,²⁰ and energetics from the literature (when available),¹² or from our calculations.

III. RESULTS

A. Integral cross sections

The integral cross sections for the reaction of CH_3CHO^+ with C_2H_2 are shown in Fig. 2 over the collision energy ($E_{\text{collision}}$) range from 0.1 to 2 eV. Product ions are observed at m/z 43 and 55 corresponding to CH_3CO^+ and $\text{C}_3\text{H}_3\text{O}^+$. These two product channels are exoergic:¹²



The latter product is identified as $\text{CH}_2\text{C(H)CO}^+$ (see Fig. 1) because that is the most stable structure of that stoichiometry. The dominant reaction channel over the whole energy range is hydrogen transfer, i.e., production of CH_3CO^+ . The ratio of the cross sections for methyl elimination to that for hydrogen transfer is just 4% at low $E_{\text{collision}}$, even though the methyl elimination channel is more energetically favorable. Methyl elimination is negligible for $E_{\text{collision}}$ above ~ 0.5 eV.

Also shown in Fig. 2 is an estimate of the collision cross section, taken as the greater of the capture cross section (σ_{capture}) or the hard sphere cross section ($\sigma_{\text{hard sphere}}$). At energies above 1 eV, σ_{capture} drops below $\sigma_{\text{hard sphere}}$ (37.8 \AA^2). The capture cross section is estimated using the statistical adiabatic channel model of Troe²¹ and the hard sphere cross section is estimated from the calculated geometries for CH_3CHO^+ and C_2H_2 . The HT reaction efficiency can be defined as the ratio of the experimental HT cross section to the collision cross section. For ground-state CH_3CHO^+ , $\sigma_{\text{HT}}/\sigma_{\text{collision}}$ is $>73\%$ at low $E_{\text{collision}}$, declining to $\sim 30\%$ at 1 eV, and remaining nearly constant at higher $E_{\text{collision}}$. The HT reaction efficiency curve is also given in Fig. 2 as a heavy dashed line. Note that at the lowest collision energy, the apparent efficiency declines slightly, deviating from the overall trend of increased efficiency with decreasing energy. This deviation is probably an artifact. As discussed below, HT produces some very slow products at low collision energies, and these may not be efficiently collected in our experiment, because of potential barriers in the ion guides. For this reason, the quoted 73% efficiency is a lower limit.

B. Velocity distributions

TOF is used to record axial velocity distributions for reactant and product ions, as described in detail elsewhere.¹

Axial velocity distributions are simply the projection of the full velocity distribution on the octapole guide axis. In our experimental geometry, the octapole is coaxial with the average relative velocity of collisions, and with the average velocity of the center-of-mass (V_{CM}). Because of this high symmetry, the axial distributions reveal much of the dynamical information contained in the full velocity distributions. For example, if reaction proceeds via a complex with lifetime (τ_{complex}) long compared to its rotational period (τ_{rotation} , typically a few picoseconds), the full velocity distribution must be isotropic in the scattering plane. The result is a forward-backward-symmetric axial velocity distribution. Conversely, a nonsymmetric axial velocity distribution is a clear sign that the reaction is not mediated by a long-lived complex, and also reveals the predominant scattering mechanism (e.g., stripping vs rebounding). Furthermore, the deviation of the velocity distribution from V_{CM} is a measure of the fraction of available energy going into recoil.

The velocity distributions for the HT and ME channels are given in Figs. 3 and 4, respectively. Distributions are shown only for the reaction of ground-state CH_3CHO^+ , but are not significantly different for the reaction of vibrationally excited reactants. Note that the velocity distributions for both product channels are forward-backward symmetric at low $E_{\text{collision}}$, but that the HT distributions become asymmetric at high energies. The trends suggest that both reactions are mediated by complexes with lifetimes greater than a picosecond at low energies, but that HT gradually becomes direct at high energies.

This is a scenario ideally suited for fitting analysis using the osculating complex model of Fisk *et al.*²² Fitting allows us to extract some quantitative information from the distributions, by accounting for experimental broadening resulting from the angular and velocity distributions of both reactants.

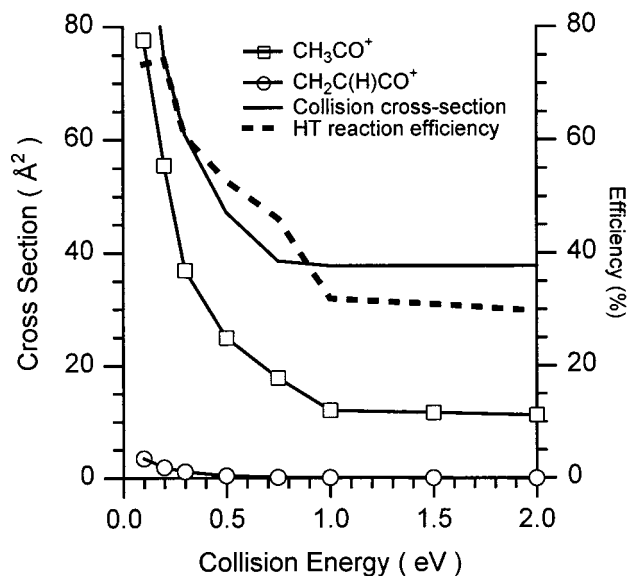


FIG. 2. Cross sections for the reaction of ground-state CH_3CHO^+ with acetylene. Also shown are the estimated collision cross section and the efficiency of the hydrogen transfer (HT) reaction.

Fitting is done using a Monte Carlo simulation of the experiment, described previously.¹ In the osculating complex model, a complex with lifetime, τ_{complex} , is assumed to form and unimolecularly decompose to products. The classical rotational period of the osculating complex, τ_{rotation} , is determined by its moment of inertia and the available angular momentum, which can be estimated from the magnitude of the cross section and collision energy. For the weakly bound complex B in Fig. 1, τ_{rotation} drops smoothly from ~ 2.1 ps at $E_{\text{collision}} = 0.15$ eV to ~ 1.2 ps at 1.32 eV. To complete the model, we also need a recoil energy distribution. $P(E_{\text{recoil}})$ is assumed to be a Gaussian peaking at $f_{\text{peak}} \cdot E_{\text{avail}}$ with width = $f_{\text{width}} / E_{\text{avail}}$:

$$P(E_{\text{recoil}}) = \exp\left(-\frac{f_{\text{width}} \cdot [E_{\text{recoil}} - f_{\text{peak}} \cdot E_{\text{avail}}]^2}{E_{\text{avail}}}\right)$$

E_{avail} is the total available energy in the products, i.e., the sum of $E_{\text{collision}}$, the reaction exoergicity and the reactant vibrational and rotational energies. $E_{\text{vibration}}$ depends on the state selected, and E_{rotation} is a thermal distribution at the scattering cell temperature (~ 350 K). The model depends on only three parameters (τ_{complex} , f_{width} , f_{peak}), all of which are physically significant.

The curves through the data points in Figs. 3 and 4 are osculating complex fits. For the HT product channel (Fig. 3) the results are as follows. At the lowest collision energy, the forward-backward-symmetric distribution suggests that τ_{complex} is longer than τ_{rotation} (2.1 ps) at 0.15 eV. As collision energy increases, the distributions become increasingly forward-peaked, with the asymmetry already beginning at 0.22 eV. At high collision energies, the distribution is fit assuming that the product peaks at 0° , and that τ_{complex} (~ 240 fs) is only $\sim 20\%$ of τ_{rotation} . It should be noted that the osculating complex model is not terribly realistic for high energy collisions because it assumes that the angular distribution is entirely due to rotation of the collision complex. In

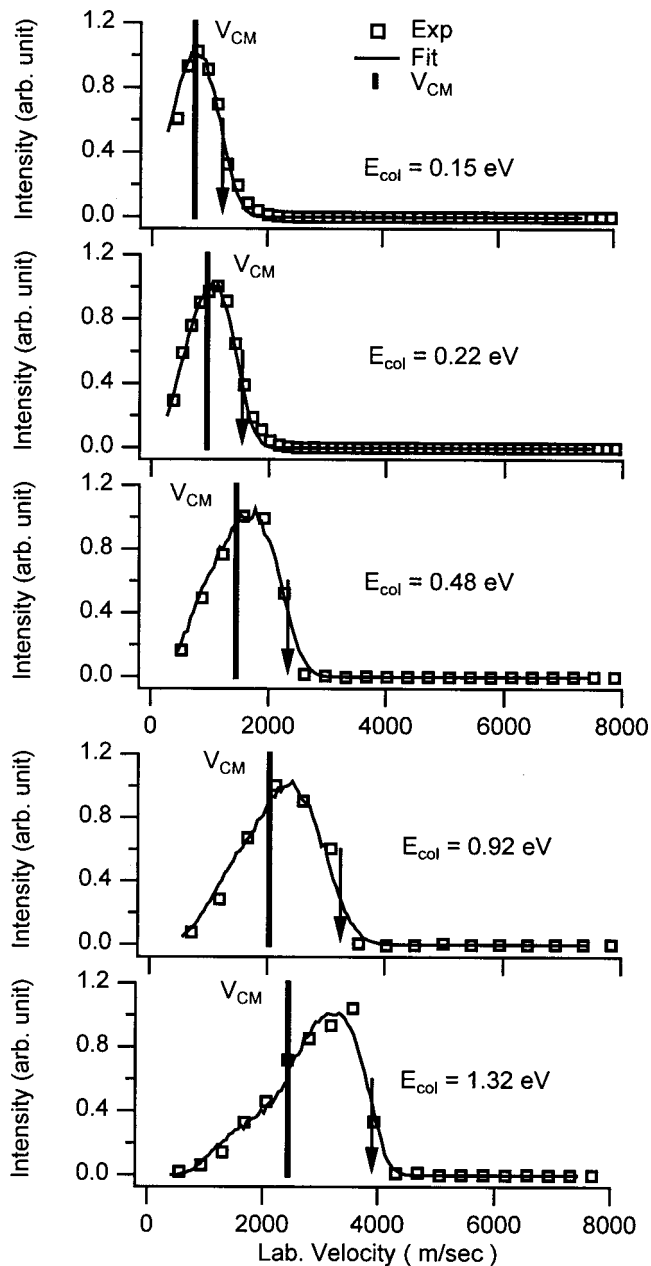


FIG. 3. Axial recoil velocity distributions for the hydrogen transfer product from the reaction of ground-state CH_3CHO^+ with C_2H_2 .

reality, the angular dependence of the scattering at high energies probably has more to do with the distribution of reactive impact parameters than the rotation of a complex. As a consequence, the τ_{complex} values at high energies are upper limits on the true collision time. The other point of interest extracted from the fits is the fraction of available energy going into recoil, $\langle E_{\text{recoil}} / E_{\text{avail}} \rangle$, summarized in Table II. At low energies, less than 10% of the available energy appears in recoil, increasing to about 25% by $E_{\text{col}} = 1.32$ eV. Also shown in Fig. 3 (as vertical arrows) are the velocities that would be expected if the system followed spectator-stripping dynamics.

Figure 4 shows recoil velocity distribution fits for the $\text{CH}_2\text{C(H)CO}^+ + \text{CH}_3$ channel and, again, the results are summarized in Table II. For this product channel, the recoil ve-

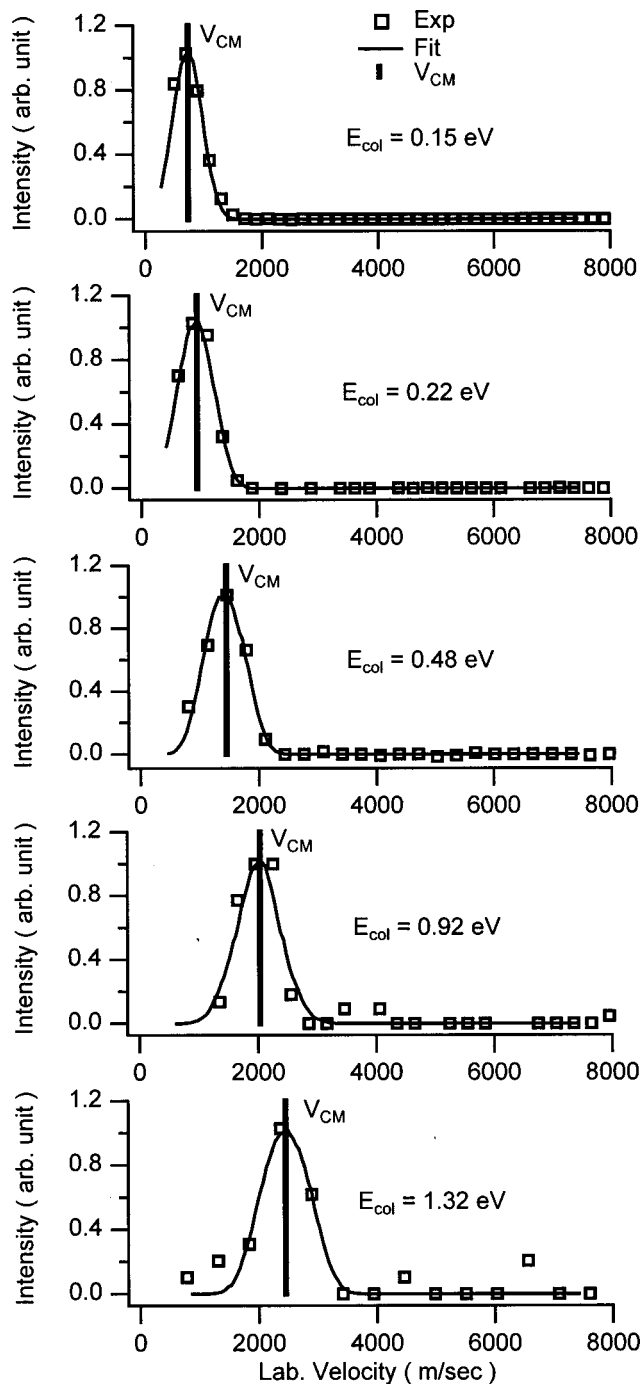


FIG. 4. Axial recoil velocity distributions for methyl-elimination product from the reaction of ground-state CH_3CHO^+ with C_2H_2 .

locity distributions are forward-backward symmetric over the entire E_{col} range. The $\langle E_{\text{recoil}}/E_{\text{avail}} \rangle$ ratios for $\text{CH}_2\text{C}(\text{H})\text{CO}^+$ are also smaller than those for HT at all energies: 7% at $E_{\text{col}}=0.15$ eV rising to 14% at $E_{\text{col}}=1.32$ eV. The difference in recoil behavior suggest that the two product channels have different mechanisms.

C. *Ab initio* results

The *ab initio* results are summarized in Fig. 1 and Table III. MP2 and B3LYP zero point energies were scaled by 0.9646 and 0.9804, respectively.²⁰ A number of covalently bound complexes were located with binding energies of 1–2.9 eV relative to reactants. In addition to the covalently bound complexes, several weakly bound “coordination” complexes, with reactantlike geometries, were found (A–C in Fig. 1). The important geometric parameters for the reactantlike complexes are listed in Table IV. The reactantlike complex C has C_2H_2 oriented so that the electron-rich triple bond is coordinated to the electron-poor oxygen atom in the CH_3CHO^+ cation. The oxygen atom is 1.45 Å away from the C atom of C_2H_2 and the carbonyl bond is only slightly lengthened (1.26 Å) relative to the bond in free CH_3CHO^+ (1.20 Å). The C–O–C angle is 126.4°. Complex B is a bridged hydrogen-bonded structure with the CHO hydrogen atom coordinated to the triple bond in C_2H_2 , with both CH–C bond lengths equal at 2.036 Å, and the C–H bond length in CHO only slightly elongated from its value (1.12 Å) in the CH_3CHO^+ cation. Complex A has the methyl group of CH_3CHO^+ coordinated to the triple bond in C_2H_2 . All heavy atoms in both moieties are coplanar, with CH_3 symmetrically disposed as shown, and the CH_3 carbon atom equidistant (3.281 Å) from the two C atoms in C_2H_2 .

For those complexes where literature energetics are available, the G3 thermal energies are consistent with the literature values to within 5 kcal/mol, except for complex J, where the G3 thermal energy is 9.4 kcal/mol higher than the value in Lias *et al.*¹² In addition, the G3 energy of the $\text{CH}_3\text{CO}^+ + \text{C}_2\text{H}_3$ product channel is 8.9 kcal/mol higher than the literature value.¹²

IV. DISCUSSION

One interesting result is the difference in cross section magnitude for the two reaction channels. The CH_3 elimination channel has just 4% efficiency at our lowest $E_{\text{collision}}$

TABLE II. Product velocity distribution fit results of CH_3CO^+ and $\text{CH}_2\text{C}(\text{H})\text{CO}^+$.

E_{col} (eV)	CH_3CO^+			$\text{CH}_2\text{C}(\text{H})\text{CO}^+$		
	E_{recoil} (eV)	$E_{\text{available}}$ (eV)	$E_{\text{recoil}}/E_{\text{available}}$ (%)	E_{recoil} (eV)	$E_{\text{available}}$ (eV)	$E_{\text{recoil}}/E_{\text{available}}$ (%)
0.15	0.15	1.56	9.4	0.12	1.76	7.0
0.22	0.18	1.63	11.3	0.17	1.84	9.4
0.48	0.29	1.89	15.3	0.26	2.10	12.1
0.92	0.48	2.33	20.6	0.36	2.54	14.1
1.32	0.69	2.73	25.2	0.42	2.94	14.1

TABLE III. Experimental and *ab initio* calculated energies relative to reactants ($\text{CH}_3\text{CHO}^+ + \text{C}_2\text{H}_2$).

Reaction energetics (eV)	mp2/6-311		b3lyp/6-311		G3 (0 K)	Experiment (Ref. 12)
	++G**	mp2/6-31G*	++G**	b3lyp/6-31G*		
$\text{C}_2\text{H}_3^+ + \text{CH}_3\text{CO}$	0.29	0.38	0.67	0.73	0.59	0.39
$\text{C}_2\text{H}_3 + \text{CH}_3\text{CO}^+$	-1.09	-1.04	-0.84	-0.87	-0.98	-1.36
$\text{C}_2\text{H}_3\text{CO}^+ + \text{CH}_3$	-1.87	-1.92	-1.39	-1.51	-1.52	-1.57
Complex A		-0.29	-0.44	-0.57	-0.29	No record
Complex B		-0.62	-0.77	-0.88	-0.47	No record
Complex C		-0.97	-0.88	-1.16	-0.95	No record
Complex D		-0.94	-0.79	-1.09	-0.83	No record
Complex E		-2.03	-2.15	-2.45	-1.64	No record
Complex F		-2.21	-2.23	-2.56	-2.11	-2.20
Complex G			-2.30	-2.68		-2.42
Complex H		-3.06	-2.23	-2.59	-2.57	-2.46
Complex I		-3.12	-3.13	-3.32	-3.04	-3.29
Complex J		-2.24	-2.31	-2.65	-2.27	-2.68
Complex K		-2.89	-2.88	-3.08	-2.87	-2.98

compared to >73% efficiency for the less energetically favorable HT channel. Another interesting observation is that we do not see two H_2 -elimination product channels (right side, Fig. 1) even though these are the most exoergic channels by a large margin. Several other exoergic product channels are also not observed. Clearly there are constraints on the reaction other than product energetics.

A. The hydrogen transfer channel

Product mass 43 is assigned to CH_3CO^+ rather than CH_2CHO^+ because production of CH_2CHO^+ is 2.1 eV endoergic,²³ and therefore inconsistent with the observation of a large cross section in our collision energy range. Similarly, we rule out significant production of CH_2COH^+ , at least for low energies, because this channel would be 0.2 eV endoergic.¹² The velocity distribution of CH_3CO^+ at our lowest collision energy (0.15 eV) is forward-backward symmetric, but the distributions become forward-peaked, beginning at quite low energies. This observation suggests that any complex that might mediate the HT reaction is weakly bound and short-lived, except at the lowest collision energies. Of the three weakly bound complexes in Fig. 1, only B has a geometry allowing transfer of the CHO hydrogen atom, and is the most likely candidate to mediate this reaction. Complexes A and C may form in the initial $\text{CH}_3\text{CHO}^+ - \text{C}_2\text{H}_2$ interaction, but must rearrange to a B-like geometry prior to reaction. Note that the short HT collision times at high energies suggests that the contribution of

CH_2COH^+ to this channel is probably not large, because CH_2COH^+ production requires rearrangement that is likely to be inefficient in fast collisions.

One obvious question is whether the lifetime of complex B is consistent with observations. For such a complex, the lifetime is determined by the rates of dissociation back to reactants combined with the rates of all processes leading forward to products. In this case, the forward process is simply an H transfer. Unfortunately, despite some effort, we have not been successful at calculating the structure of the transition state connecting complex B to the products (labeled TS2 in Fig. 1). TS2 is clearly below the energy of the reactants, but its energy and tightness are unknown. The only rate we are able to calculate is, therefore, the rate of complex B dissociation back to reactants. This calculation was done using an orbiting TS²⁴ for the dissociation, and the *ab initio* frequencies and moments of inertia for the complex. The lifetimes with respect to dissociation only, i.e., upper limits on the true lifetimes, are summarized in Table V. At the lowest energy, the lifetime is long compared to τ_{rotation} , consistent with the observation of forward-backward symmetry in the velocity distribution. The lifetime that can be supported by complex B drops very rapidly with increasing energy, again consistent with the observation of a transition to direct dynamics at low collision energy.

The efficiency of this reaction ranges from >73% at low energies to ~30% at high energies. The efficiency at high energies is about what one might expect from steric con-

TABLE IV. Selected distances and angles of reactant-like complexes as results of *ab initio* calculations.

	Complex A		Complex B		Complex C	
angle C1 ^a -c ^b -C2 ^a	21.5°		angle C2-h ^b -C1	34.6°	angle C2-C1-o ^b	117.3°
distance C1-c	3.281 Å		distance C1-h	2.036 Å	angle C1-o-c	126.4°
distance C2-c	3.281 Å		distance C2-h	2.036 Å	distance C1-o	1.453 Å
distance C1-C2	1.22 Å		distance C1-C2	1.211 Å	distance c-o	1.261 Å
			distance c-h	1.17 Å	distance C1-C2	1.298 Å

^aUpper case "C" refers to carbon atoms of the C_2H_2 moiety.

^bLower case c, h, and o refer to the CHO atoms in CH_3CHO^+ .

TABLE V. Fit collision times and RRKM complex lifetimes.

E_{col} (eV)	Expt. ^a (ps)	Expt. ^b (ps)	RRKM (com. B) ^c (ps)	RRKM (com. J) ^d (ps)	RRKM (com. J) ^e (ps)	Direct collision ^f (ps)
0.15	>2.1	>1.9	11.5	<0.1 ^g	<0.1	0.43
0.22	1.1	>1.8	1.28	<0.1	<0.1	0.33
0.48	0.7	>1.7	<0.1	<0.1	<0.1	0.22
0.92	0.4	>1.5	<0.1	<0.1	<0.1	0.15
1.32	0.2	>1.5	<0.1	<0.1	<0.1	0.13

^aCH₃CO⁺ recoil velocity distribution fits.

^bCH₂C(H)CO⁺ recoil velocity distribution fits.

^cDissociation from complex B to reactants (CH₃CHO⁺+C₂H₂).

^dDissociation from complex J to products (CH₃CO⁺+C₂H₃).

^eDissociation from complex J to products (CH₂C(H)CO⁺+CH₃).

^fTime for reactants to traverse 5 Å.

^gLifetime below limit where RRKM is expected to be valid.

straints, i.e., the requirement that the C₂H₂ reactant must interact in the correct orientation with a transferable H atom on CH₃CHO⁺. The substantial increase in efficiency at low energies implies that collisions in unfavorable initial geometries must be able to reorient to some degree. The only forces acting to orient the reactants at long range are weak. C₂H₂ will tend to orient with its molecular axis toward the center-of-charge on CH₃CHO⁺ (i.e., unfavorably), because its polarizability is roughly four times greater in that orientation. CH₃CHO⁺ also feels an orienting force, resulting from the fact that its center-of-charge (i.e., center of the main attractive force) is displaced from its center-of-mass. The center-of-mass for CH₃CHO⁺ is indicated by a point labeled ‘‘M’’ in the inset at the lower right corner of Fig. 1. The center-of-charge is the point labeled with a ‘‘(+’’ sign. There is a net torque roughly about the CC axis of CH₃CHO⁺ tending to rotate the aldehyde H atom toward the approaching C₂H₂, i.e., into the reactive geometry. Still, for these relatively heavy reactants, reorientation during reactant approach is not significant at the collision energies in our experiments. For example, if we calculate the torque on CH₃CHO⁺ at a reactant separation of 5 Å, with reactants oriented to give the maximum torque, the angular acceleration is such that it would take 0.4 ps to reorient by 20°. In comparison, even at $E_{\text{collision}}=0.15$ eV, it only takes ~100 fs for the reactants to approach from 5 Å to the hard sphere contact distance (3.5 Å), suggesting that reorientation during approach is not a significant effect. Of course, choice of a longer characteristic distance would increase the interaction time, but as the interaction falls off like R^{-4} , significant torques only occur at short range.

Instead, we propose that the increase in reaction efficiency is attributable to the reactantlike complexes A and especially C, which can form in collisions with unfavorable geometries. These complexes have the wrong geometries to allow aldehyde H transfer, but may rearrange into geometries similar to that of complex B, where HT can occur. Again, we do not have the transition state information to calculate the lifetimes of complexes A and C, but C presumably has a substantial lifetime. To the extent that the ‘‘reactants→complex C→complex B→products’’ mechanism is important, it provides an alternative route to products

at low energies (increasing the reaction efficiency) and also increases the time scale of the HT collisions.

B. The methyl-elimination channel

The methyl-elimination channel gives forward-backward-symmetric velocity distributions at all energies, and also partitions less energy into recoil of the products than the HT channel (Table II). Both factors suggest that the mechanism for this channel involves longer collision times, allowing more extensive energy transfer. This requirement is not surprising. Methyl-elimination to generate the low energy CH₂C(H)CO⁺ product requires extensive rearrangement, including CC bond formation, a net hydrogen shift by two positions on the carbon backbone, followed by methyl-elimination. While there may be other conceivable reaction paths, one suggested by our calculations is ‘‘reactants→complex B→TS1→complex J→products.’’ Complex J is quite productlike, and as such, the system almost has to pass through such a configuration. Similarly, the system must almost certainly pass through a geometry similar to that of complex B on the way to forming the new CC bond in complex J. Note, however, that the concerted, four-center isomerization through TS1 is hypothetical, and the transformation from B to J may, instead, proceed by a multistep process.

There are two other complexes more stable than complex J, i.e., complex I and complex K. We can completely rule out any participation of the most stable complex, I, based on the observed product distribution. Complex I has been prepared from a stable neutral precursor, and its collisionally activated decomposition-mass-analyzed ion kinetic energy (CAD-MIKE) spectrum has been reported.²⁵ In CAD-MIKE, as in our experiments, ground electronic state, collisionally activated complexes are prepared. If complex I were formed in our experiments, our product distribution should include all the main fragment ions observed in the CAD-MIKE spectrum. In CAD-MIKE of complex I, the main ion fragments are at masses 42 and 39, which are completely absent in our product ion distribution. On the other hand, CAD-MIKE of ions with structures corresponding to com-

plex J and complex $\text{K}^{25,26}$ is dominated by fragment ions at masses 43 and 55, i.e., the same products that we observe. It is clear, however, that our product distribution does not result *only* from the decomposition of complexes J and K, because those complexes primarily fragment by CH_3 elimination (>75% of the total fragments), while CH_3 elimination is a minor channel in the reaction of CH_3CHO^+ with C_2H_2 . This observation is consistent with the conclusion above, i.e., the reaction leading to mass 43 (the HT reaction) is mostly a direct reaction, not mediated by a covalently bound complex. The CAD-MIKE spectra also suggest that complex K may participate in mediating the CH_3 elimination reaction. We note, however, that complex K can only eliminate CH_3 by first rearranging to complex J, supporting our conclusion that the reaction coordinate must pass through complex J. The fact that K eliminates CH_3 in CAD-MIKE indicates that $\text{J} \rightleftharpoons \text{K}$ isomerization is facile.

When strongly bound complexes such as J or K exist, and the reaction clearly is mediated by a long-lived complex, it is natural to assume that these complexes are responsible for the long lifetime. In reality, the situation is more complicated. We have estimated the RRKM lifetimes of complex J with respect to dissociation to both product channels, assuming orbiting transition states²⁷ in the exit channels, with angular momentum given by the average angular momentum in the collisions. As both channels involve ion-radical separation, it is highly unlikely that there are activation barriers other than the centrifugal barrier. The situation for complex K is probably similar, but more complicated because K must rearrange to J before dissociating to products. The results are given in Table V, together with the complex lifetime inferred from the osculating complex model fits to the velocity distributions, and the lifetime of complex B with respect to dissociation back to reactants.

The lifetimes of complex J with respect to the sum of HT and methyl-elimination rates are shorter than 100 fs at all energies. (We regard 100 fs as a minimum time scale, below which the ergodic assumption of the RRKM model is unreasonable.) The short lifetime is a consequence of the fact that even at zero collision energy, there is substantial excess energy with respect to these exoergic product channels. Negligible lifetime in complex J is certainly consistent with the direct dynamics observed for HT, and indicates that the longer lifetimes observed at very low energies must be the result of time spent in the reactantlike complex B (perhaps in combination with C). The short lifetime of complex J appears inconsistent, however, with the conclusion that methyl-elimination proceeds through a long-lived complex at all collision energies.

There are two possible resolutions to this discrepancy, both based on the idea that the slow step in the methyl-elimination reaction mechanism comes prior to the formation of complex J. One possibility is that the rate of passage from B to J via TS1 is slow, and the collision time is largely spent in reactantlike complexes. As the table shows, these complexes also have short lifetimes at higher energy, and this mechanism essentially says that the methyl-elimination channel is open only to the long-time tail of the lifetime distribution for the reactantlike complexes. This scenario

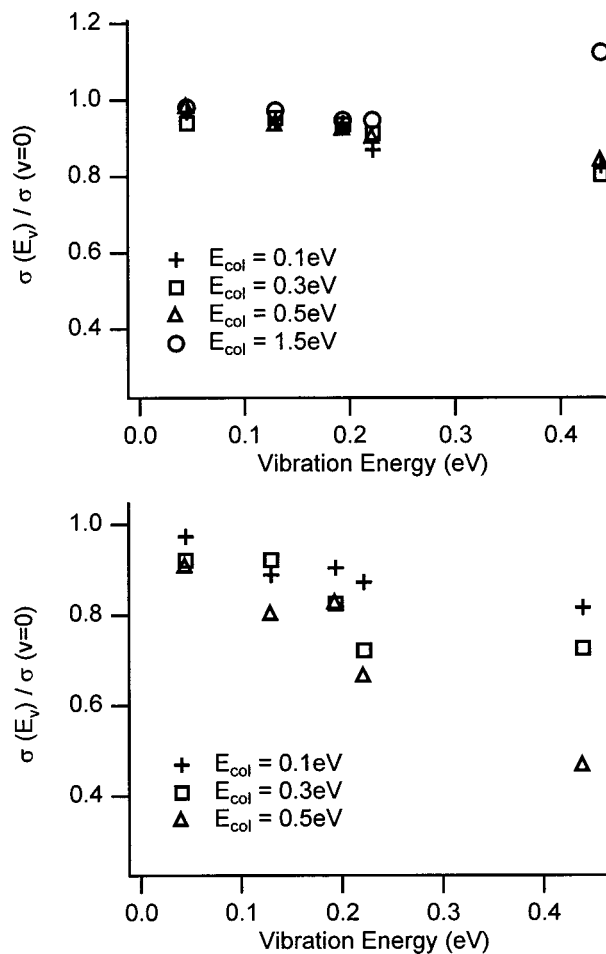


FIG. 5. Vibrational effects on the hydrogen transfer and methyl-elimination channels (top and bottom frames, respectively). Ratios of the cross section for reaction of various vibrational states to the cross section for reaction of ground-state CH_3CHO^+ are plotted.

would imply that the fraction of reactantlike complexes that survives long enough to contribute to the methyl-elimination channel should become very small at high collision energies, consistent with the observed strong inhibition of this channel by energy. Alternatively, it is possible that the $\text{B} \rightarrow \text{J}$ isomerization goes through one or more intermediate complexes, and that these complexes account for the long time scale of collisions leading to methyl-elimination. Without detailed information on all the transition states connecting these complexes, we are not able to be more definite about the mechanism.

C. Vibrational effect

Figure 5 shows the effects of CH_3CHO^+ vibrational energy on the cross sections for the HT and methyl-elimination reactions at low collision energies, plotted as the ratio of the cross section for excited CH_3CHO^+ to the cross section for reaction of the ground state. For HT (top frame) there is a weak inhibition from vibration, proportional to the vibrational energy within experimental error. The weak effect of vibration is in contrast to the strong inhibition from collision energy. Adding 0.44 eV of vibrational energy results in a ~17% drop in the HT cross section at low collision

energies—only one-quarter of the effect from adding the same amount of collision energy. It is particularly interesting that ν_3 , dominating the motion for the point at $E_{\text{vib}}=0.44$ eV, has such a small effect. This vibration is the aldehyde CH stretch, i.e., a high energy stretch of the bond being broken in HT. Simple considerations would suggest that this vibration is strongly coupled to the reaction coordinate, and therefore should have a substantial effect. At collision energies above 1 eV, there is a small ($\sim 15\%$) apparent enhancement from the ν_3 vibration. The uncertainty for this state is large ($\sim 15\%$) because of very low beam intensity, but even if real, the effect is small considering the nature of the vibration.

The vibrational effects are somewhat larger for the methyl-elimination channel, particularly at high collision energies. Within experimental error, the vibrational effects are proportional to vibrational energy, i.e., there are no mode-specific effects. At our lowest collision energies, the methyl-elimination channel is inhibited $\sim 20\%$ by adding 0.44 eV of vibrational energy, compared to $\sim 90\%$ inhibition from adding the same amount of collision energy. At $E_{\text{collision}}=0.5$ eV, there is $\sim 50\%$ inhibition from adding 0.44 eV of vibrational energy, compared to $\sim 75\%$ inhibition from adding 0.5 eV of collision energy.

Adding collision energy is fundamentally different from adding vibrational energy, because there is substantial angular momentum associated with the collision energy. In a reaction mediated by a long-lived complex, branching between the decay of the complex to products versus decay back to reactants can often be strongly dependent on angular momentum. Consider, for example, the ‘‘reactant \rightarrow B \rightarrow J \rightarrow products’’ mechanism proposed above for the methyl-elimination channel. When a complex such as B forms, a significant fraction of the available energy must go into the tumbling rotation of the complex in order to conserve angular momentum ($E_{\text{rot}}=L^2/2I$, where I is the moment of inertia for tumbling). In this case, complex B can decay through an orbiting TS back to reactants, or on to products through the lower energy, but tighter TS1. Because TS1 is more compact than complex B, the fraction of available energy tied up in tumbling rotation must increase, i.e., the energy available to drive the transition decreases with increasing L . In contrast, the orbiting TS leading back to reactants is less compact than the complex, thus some of the tumbling energy is made available to drive dissociation. In sum, increasing collision energy, and thus increasing L , tends to favor dissociation back to reactants. Vibrational energy, because it has no associated angular momentum, should increase the available energy at both transition states equally.

The fact that methyl-elimination is inhibited by vibration, but not as much as by equivalent amounts of collision energy, is consistent with this reaction being mediated by a long-lived complex, with the rate-limiting step being isomerization out of complex B, as proposed above. TS1 not only has a smaller moment of inertia than the orbiting TS for dissociation, but it is also certainly much tighter. Adding energy of any form will tend to favor complex decay via the looser TS (i.e., favor dissociation to reactants), but adding collision energy has the additional effect of angular momen-

tum, also favoring dissociation back to reactants.

The observation of only a weak vibrational effect on HT at high collision energies is not surprising. HT is direct in this energy regime, and apparently none of the CH_3CHO^+ vibrations significantly affect the direct hydrogen transfer process. Note that, at high energies, $E_{\text{collision}}$ also has little effect on HT efficiency. As discussed above, the conclusion is that the HT reaction is primarily dependent on the collision geometry at high collision energies, and neither vibration nor collision energy has much effect.

At low collision energies, HT efficiency is enhanced by the formation of weakly bound collision complexes (e.g., ‘‘B’’ in Fig. 1) that provide time for reactants to reorient from unfavorable to reactive geometries. The strong effect of collision energy at low energies is a consequence of the reduced lifetime of intermediate complexes. The fact that vibration has less of an effect than collision energy is attributable to the fact that vibration simply adds energy to the system, while increasing collision energy also increases the angular momentum.

HT has a weaker dependence on both collision and vibrational energy than methyl-elimination, which presumably reflects the fact that the two reactions go by different mechanisms. Both channels probably pass through a ‘‘B’’-like complex, which can directly decay to HT products via TS2, or can rearrange through covalently bound geometries (e.g., ‘‘J’’ via TS1. In this scenario, the differences in vibrational and collision energy effects must relate to the differences between TS1 and TS2. The implication is that TS2 (mediating HT) is looser than TS1 (mediating methyl-elimination), so that HT competes more effectively with dissociation back to the reactants as the energy and angular momentum are increased. The reaction coordinate for HT is simply a hydrogen atom transfer, and TS2 should be quite loose. TS1 must allow CC bond formation and H migration, and must be substantially tighter.

ACKNOWLEDGMENT

This work was supported by the National Science Foundation under Grant No. CHE-9807625.

- ¹Y.-H. Chiu, H. Fu, J.-T. Huang, and S. L. Anderson, *J. Chem. Phys.* **102**, 1199 (1995).
- ²Y.-H. Chiu, H. Fu, J.-T. Huang, and S. L. Anderson, *J. Chem. Phys.* **105**, 3089 (1996).
- ³J. Qian, H. Fu, and S. L. Anderson, *J. Phys. Chem.* **101**, 6504 (1997).
- ⁴H. Fu, J. Qian, R. J. Green, and S. L. Anderson, *J. Chem. Phys.* **108**, 2395 (1998).
- ⁵J. Qian, R. J. Green, and S. L. Anderson, *J. Chem. Phys.* **108**, 7173 (1998).
- ⁶R. J. Green, H.-T. Kim, J. Qian, and S. L. Anderson, *J. Chem. Phys.* **113**, 4158 (2000).
- ⁷S. J. Klippenstein, *J. Chem. Phys.* **104**, 5437 (1996).
- ⁸Q. Cui, Z. Liu, and K. Morokuma, *J. Chem. Phys.* **109**, 56 (1998).
- ⁹Q. Cui and K. Morokuma, *J. Chem. Phys.* **108**, 4021 (1998).
- ¹⁰S. Irle and K. Morokuma, *J. Chem. Phys.* **111**, 3978 (1999).
- ¹¹H.-T. Kim and S. L. Anderson, *J. Chem. Phys.* **114**, 3018 (2001).
- ¹²S. G. Lias, J. E. Bartmess, J. F. Liebman, J. L. Holmes, and R. D. Levin, *J. Phys. Chem. Ref. Data Suppl.* **17**, 1 (1988).
- ¹³M. J. Frisch, G. W. Trucks, H. B. Schlegel *et al.*, GAUSSIAN 98, Gaussian, Inc., Pittsburgh, PA, 1998.
- ¹⁴H. W. Jochims, W. Lohr, and H. Baumgartel, *Chem. Phys. Lett.* **54**, 594 (1978).

- ¹⁵F. Turecek and V. Hanus, *Org. Mass Spectrom.* **19**, 423 (1984).
- ¹⁶Y. Apeloig, M. Karni, B. Ciommer, G. Depke, G. Frenking, S. Meyn, J. Schmidt, and H. Schwarz, *Int. J. Mass Spectrom. Ion Processes* **59**, 21 (1984).
- ¹⁷W. J. Bouma, J. K. MacLeod, and L. Radom, *J. Am. Chem. Soc.* **101**, 5540 (1979).
- ¹⁸G. Bouchoux, J. P. Flament, and Y. Hoppilliard, *Int. J. Mass Spectrom. Ion Processes* **57**, 179 (1984).
- ¹⁹L. Zhu and W. L. Hase, *Quant. Chem. Prog. Exchange*, QCPE 644.
- ²⁰J. B. Foresman and A. Frisch, *Exploring Chemistry with Electronic Structure Methods*, 2nd ed. (Gaussian, Pittsburgh, 1993).
- ²¹J. Troe, *Chem. Phys. Lett.* **122**, 425 (1985).
- ²²G. A. Fisk, J. D. McDonald, and D. R. Herschbach, *Discuss. Faraday Soc.* **44**, 228 (1967).
- ²³R. H. Nobes, W. J. Bouma, and L. Radom, *J. Am. Chem. Soc.* **105**, 309 (1983).
- ²⁴M. T. Rodgers, K. M. Ervin, and P. B. Armentrout, *J. Chem. Phys.* **106**, 4499 (1997).
- ²⁵S. Arseniyadis, J. Gore, P. Guenot, and R. Carrie, *J. Chem. Soc., Perkin Trans. 2* **1985**, 1413 (1985).
- ²⁶J. K. Terlouw, W. Heerma, J. L. Holmes, and P. C. Burgers, *Org. Mass Spectrom.* **15**, 582 (1980).
- ²⁷M. T. Rodgers and P. B. Armentrout, *J. Chem. Phys.* **109**, 1787 (1998).